JOC*Article*

Toward an Amphiphilic Bilirubin: The Crystal Structure of a Bilirubin *E*-Isomer

Sanjeev K. Dey and David A. Lightner*

Department of Chemistry, University of Nevada, Reno, Nevada 89557

lightner@scs.unr.edu

Received December 6, 2007

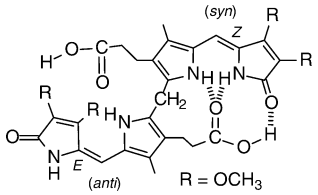

A new bilirubinoid analog (**1**) with two methoxy β-substituents on the lactam ring of each dipyrrinone was synthesized and examined spectroscopically. It is more soluble in CH_3OH and $CHCl_3$ than bilirubin, which is insoluble in CH_3OH but soluble in $CHCl_3$. The solubility of **1** is ~10 μg/mL in CH_3OH (vs $\leq$1 μg/mL for bilirubin) and ~3 mg/mL in $CHCl_3$ (vs ~0.6 mg/mL for bilirubin). Vapor pressure osmometry indicates that **1**, like bilirubin, is monomeric in $CHCl_3$, and NMR studies show that the most stable structure has the *syn*-4*Z*,*syn*-15*Z* configuration, with the pigment's dipyrrinones engaged in intramolecular hydrogen bonding to the propionic acid carboxyl groups. And, like bilirubin, *Z*,*Z*-**1** adopts a conformation that is bent in the middle into a ridge-tile shape. For the first time, a crystal structure of a bilirubin *E*-isomer has been obtained. Crystallization of **1** under dim room lighting gave an X-ray quality crystal of the *anti*-4*E*,*syn*-15*Z*-(photo) isomer, in which only the *Z*-dipyrrinone half is engaged in intramolecular hydrogen bonding to a propionic acid. Hydrogen bonding is nearly completely disengaged in the *E*-dipyrrinone half; yet, the ridge-tile conformation persists.

Introduction

Bilirubin (Figure 1A), the end product of heme metabolism in mammals,[1] is a lipophilic tetrapyrrole dicarboxylic acid,[2] the yellow neurotoxic pigment of jaundice,[1,2] and a powerful antioxidant.[3] Bilirubin and its blue-green biogenetic precursor, biliverdin, are formed copiously in healthy humans by catabolism of heme and other heme proteins, and they are eliminated from circulation by the liver, crossing into bile.[1,4] Unlike biliverdin, which is polar and excreted intact across the liver, bilirubin is nonpolar and requires glucuronidation of at least one propionic acid group for transhepatic transport.[1,4] Some 65 years ago, Hans Fischer determined their constitutional structures by degradation methods and total synthesis and indicated linear structures for the pigments without designating the configurational stereochemistry of the exocyclic C=C bonds[5] at C(4), C(10) and C(15). Lemberg[6] suggested that an all-*Z* configuration would follow logically from the porphyrin precursor; yet, he used "linear" representations in his classic (1949) book[7] with Legge, apparently because they "save space and are more readily visualized." Thus, from the late 1930s to present times linear structural representations of bilirubin and biliverdin (Figure 1B) have persisted in the literature and biochemistry texts—often

(1) Chowdhury, J. R.; Wolkoff, A. W.; Chowdhury, N. R.; Arias, I. M. Hereditary jaundice and disorders of bilirubin metabolism. In *The Metabolic and Molecular Bases of Inherited Disease*; Scriver C. F., Beaudet A. L, Sly W. S., Valle D., Eds.; McGraw-Hill: New York, 2001; Chapter 125, pp 3063−3101.

(2) (a) Lightner, D. A.; McDonagh, A. F. *Acc. Chem. Res.* **1984**, *17*, 417−424. (b) McDonagh, A. F.; Lightner, D. A. *Pediatrics* **1985**, *75*, 443−455. (c) McDonagh, A. F.; Lightner, D. A. *Semin. Liver Dis.* **1988**, *8*, 272−283.

(3) (a) Dore, S.; Takahashi, M.; Ferris, C. C.; Hester, L. D.; Guastella, D.; Snyder, S. H. *Proc. Natl. Acad. Sci.* **1999**, *96*, 2445−2450. (b) Stocker, S.; Yamamoto, Y.; McDonagh, A. F.; Glazer, A. N.; Ames, B. N. *Science* **1987**, *235*, 1043−1046.

(4) (a) McDonagh, A. F. Bile pigments: Bilatrienes and 5,15-biladienes. In *The Porphyrins*; Dolphin D., Ed.; Academic Press: New York, 1979; Vol VI, Chapter 6. (b) Schmid, R.; McDonagh, A. F. Hyperbilirubinemia. In *The Metabolic Basis of Inherited Disease*, 4th ed.; Stanbury, J. B., Wyngaarden, J. B., Fredrickson, D. S., Eds.; McGraw-Hill: New York, 1978; pp 1221−1257.

(5) Fischer, H.; Plieninger, H. *Hoppe-Seyler's Z. Physiol. Chem*. **1942**, *274*, 231−260.

(6) Lemberg, R. *Austral. Chem. Int. J. Proc*. **1939**, *6*, 170−180.

(7) Lemberg, R.; Legge, J. W. *Hematin Compounds and Bile Pigments*; Interscience Publ., Inc.: New York, 1949.

10.1021/jo702593x CCC: $40.75
Published on Web 03/08/2008

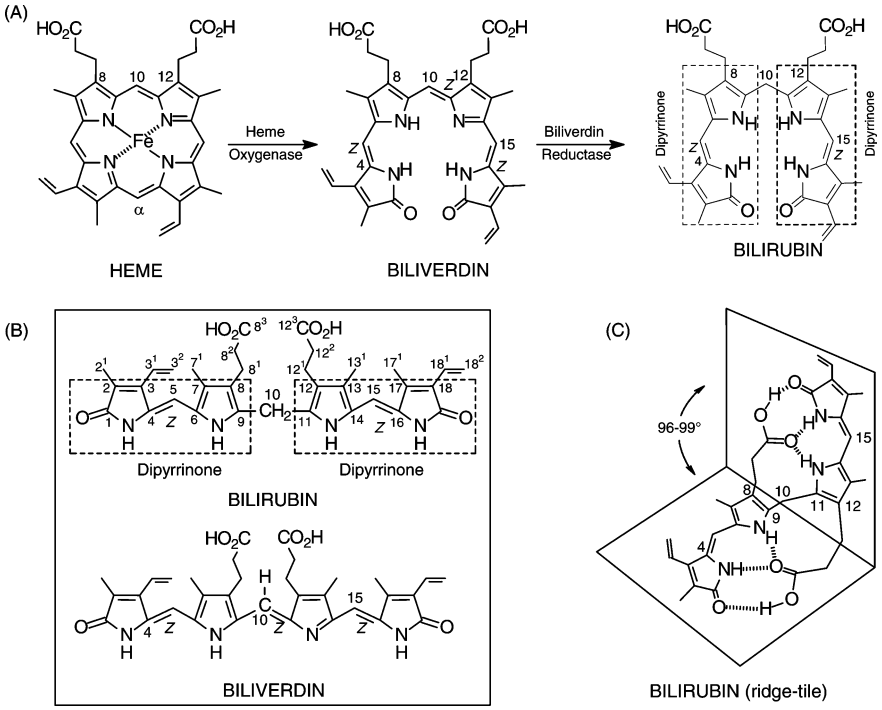

FIGURE 1. (A) Catabolism of heme to biliverdin and bilirubin, both shown in porphyrin-like representations. The most stable conformation of biliverdin is porphyrin-like and helical. (B) Linear representations of biliverdin and bilirubin, both unstable conformations. (C) The most stable conformation of bilirubin is neither linear nor porphyrin-like but folded into a half-opened book or ridge-tile shape that is stabilized by 6 intramolecular hydrogen bonds. (Only one enantiomer is shown.)

with the wrong double bond stereochemistry. The double bond configuration was clarified as *Z* approximately 30 years ago by X-ray crystallography,[8,9] and we now know that (4*Z*,10*Z*,15*Z*)-verdins adopt a porphyrin-like conformation while the most stable conformation of (4*Z*,15*Z*)-rubins is neither linear or porphyrin-like.[10] In bilirubin the two dipyrrinones may in principle rotate freely about the central 10-CH_2 like propeller blades to generate a multitude of conformations, of which the linear and porphyrin-like are highest energy and one resembling a half-opened book (Figure 1C) minimizes intramolecular nonbonded steric repulsions.[11]

It is in such a "ridge-tile" shape[9] that bilirubin is further stabilized by intramolecular hydrogen bonding between the propionic acid COOH groups and the opposing dipyrrinone lactam and pyrrole groups (Figure 1C),[9,11] a conformation that explains its polarity and solubility that differs from biliverdin: insoluble in CH_3OH (biliverdin is soluble) and solubility in $CHCl_3$ (biliverdin is insoluble).[2] It also explains bilirubin's lipophilicity and correlates with the pigment's inability to be excreted intact by the liver.[12] However, when some of the hydrogen bonds are broken, as in the *E*-isomers of bilirubin formed during phototherapy for jaundice in the newborn,[2] or in adults exposed to natural light,[13] the pigment can be excreted intact — and glucuronidated at the propionic acid still engaged in intramolecular hydrogen bonding. Although X-ray crystal structures of natural 4*Z*,15*Z*-bilirubin[9] and some of its synthetic analogs have been obtained,[8,14] no crystal structures of a bilirubin *E*-isomer have been reported.

Bilirubin *E*-isomers are important because by breaking a set of intramolecular hydrogen bonds, the pigment becomes more polar and excretable,[2,15] which is of fundamental importance to the success of the widely used phototherapy for the jaundiced newborn.[1,2] Earlier, we explored the influence of non-ionizable substituents on the lipophilicity of bilirubins in which intramolecular hydrogen bonding is maintained. Thus, we designed and synthesized analogs that were capable of intramolecular hydrogen bonding but were either more or less lipophilic than bilirubin by: (1) changing the lactam β-substituents from methyl and vinyl to two ethyls,[16] or to a methyl and *n*-butyl,[17] which increased the pigment's lipophilicity; (2) adding a *gem*-dimethyl group to C(10), which increased the pigment's solubility in nonpolar as well as polar (e.g., CH_3OH) solvents;[16a] and (3) synthesizing analogs with α-F or α-OCH_3 groups on the

(8) (a) Sheldrick, W. S. *Israel J. Chem.* **1983**, *23*, 155−166. (b) Sheldrick, W. S. *J. Chem. Soc., Perkin 2* **1976**, 1457−1462.

(9) (a) Bonnett, R.; Davies, J. E.; Hursthouse, N. B.; Sheldrick, G. M. *Proc. R. Soc. London, Ser. B* **1978**, *202*, 249−268. (b) LeBas, G.; Allegret, A.; Mauguen, Y.; DeRango, C.; Bailly, M. *Acta Crystallogr.* **1980**, *B36*, 3007−3011. (c) Becker, W.; Sheldrick, W. S. *Acta. Crystallogr., Sect. B* **1978**, *B34*, 1298−1304. (d) Mugnoli, A.; Manitto, P.; Monti, D. *Acta Crystallogr.* **1983**, *C39*, 1287−1291.

(10) Falk, H. *The Chemistry of Linear Oligopyrroles and Bile Pigments*; Springer-Verlag: Wien, 1989.

(11) Person, R. V.; Peterson, B. R.; Lightner, D. A. *J. Am. Chem. Soc.* **1994**, *116*, 42−59.

(12) (a) McDonagh, A. F.; Lightner, D. A. *Cell. Mol. Biol.* **1994**, *40*, 965−974. (b) McDonagh, A. F.; Lightner, D. A.; Nogales, D. F.; Norona, W. *FEBS Lett.* **2001**, *506*, 211−215.

(13) McDonagh, A. F. *N. Engl. J. Med.* **1986**, *314*, 121−122.

(14) (a) Ghosh, B.; Catalano, V. J.; Lightner, D. A. *Monatsh. Chem.* **2004**, *135*, 1305−1317. (b) Tipton, A.; Lightner, D. A. *Monatsh. Chem.* **2002**, *133*, 707−716. (c) Kar, A. K.; Tipton, A. K.; Lightner, D. A. *Monatsh. Chem.* **1999**, *130*, 833−843.

(15) McDonagh, A. F.; Lightner, D. A. *Semin. Liver Dis.* **1988**, *8*, 272−283.

(16) (a) Xie, M.; Holmes, D. L.; Lightner, D. A. *Tetrahedron* **1993**, *49*, 9235−9250. (b) Ghosh, B.; Lightner, D. A.; McDonagh, A. F. *Monatsh. Chem.* **2004**, *135*, 1189−1999.

(17) Brower, J. O.; Lightner, D. A.; McDonagh, A. F. *Tetrahedron* **2000**, *56*, 7869−7883.

propionic acid chains,[18] which increased the pigment's polarity and decreased its lipophilicity—even making the former water-soluble. In our quest to obtain a truly amphiphilic bilirubin, more recently we synthesized a water-soluble bilirubin attached to polyethyleneglycol (PEG), where the pigment's intramolecular hydrogen bonding ability and intrinsic lipophilicity remained unperturbed.[19] However, except at pH <10, it was found to be aggregated, probably with the pigment aggregate sequestered in the core of a PEG micelle. In a quest for water-soluble, non-ionic and nonaggregated bilirubin analogs, we initiated the syntheses of bilirubins with ether and polyether β-substituents and report herein the preparation of 2,17-desmethyl-3,18-desvinyl-2,3,17,18-tetramethoxybilirubin (**1**), which we call tetramethoxybilirubin (and its diethyl ester, **1e**), with β-methoxy groups on the lactam rings (**1**, Structures). Its properties are compared to those of the tetraethyl analog 2,17-desmethyl-3,-18-desvinyl-2,3,17,18-tetraethylbilirubin (which we call tetraethylbilirubin, **2,** Structures), its diethyl ester (**2e**), and bilirubin. Unexpectedly, crystallization of 4*Z*,15*Z*-**1** in dim room lighting produced X-ray quality crystals of its *E*,*Z* isomer, and in the following we also report the first crystal structure of a bilirubin *E*-configuration isomer.

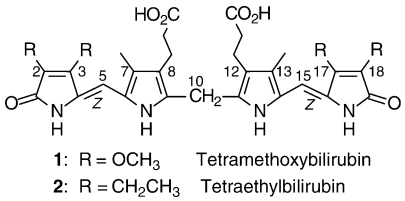

Results and Discussion

Synthesis. From our perspective the simplest route to the preparation of methoxyrubin **1** was to follow the "1+2+1" approach outlined in Scheme 1, where an α,α'-diformyldipyrrylmethane is coupled with two equivalents of a pyrrolin-2-one.[20] Typically, the first condensation product is a tripyrrole aldehyde intermediate, the "1+2" product, which reacts further to give the tetrapyrrole. The strategy has been used successfully in the syntheses of various end ring-modified bilirubins[16,17,19,21,22] and 10-oxo-bilirubin.[21] For the syntheses, the required dipyrrole dialdehyde (**3**) had been reported previously;[17] **4** was also known from earlier work in our lab,[23] as was **5**.[16] Condensation of dimethoxypyrrolinone **4** with **3** in refluxing methanolic KOH afforded **1** in 46% isolated yield, based on recovered tripyrrole intermediate. Similarly, diethylpyrrolinone **5** was condensed with **3** to yield **2** in 67% isolated yield, based on recovered tripyrrole intermediate. Using the same "1+2+1" approach,[20] the corresponding diethyl esters, **1e** and **2e**, were prepared from the same components, using phosphazene P_1-*t*-butyl base in toluene at reflux (for **2e**) or DBU in CH_3CN-toluene at 120−140 °C (sealed tube) (for **1e**).

SCHEME 1

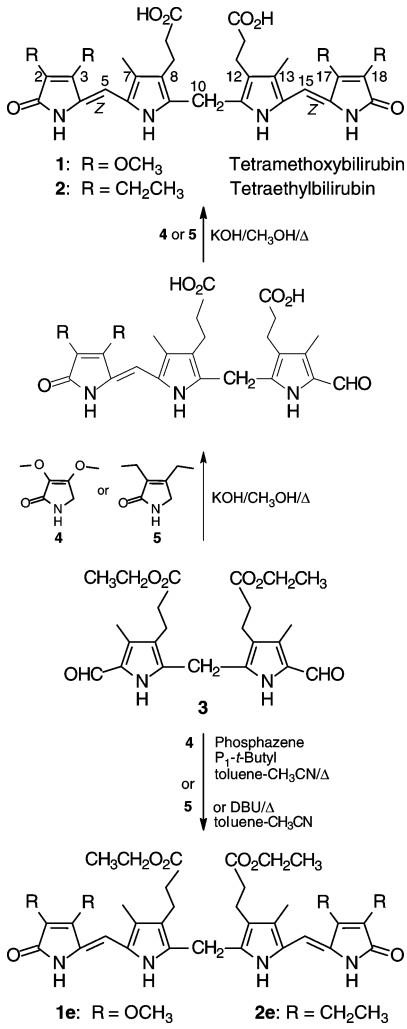

Structure. The constitutional structures of **1** and **2**, **1e** and **2e** follow from the method of synthesis (Scheme 1) and from their ^{13}C NMR spectra (Table 1). When compared with ^{13}C NMR data from the known mesobilirubin-XIIIα,[17] the various carbons of the dipyrrinone(s) of **2** have counterparts with recognizably similar chemical shifts. Major differences between **1** and **2** are found in the more shielded lactam ring carbons 1, 2 and 4 and C(5) of **1** relative to **2**, the absence of the 2^1,3^1,17^1 and 18^1 CH_2 groups in **1** and its deshielded 2^2,3^2,17^2,18^2 CH_3 groups. Aside from the prominently deshielded OCH_3 groups of **1**, the ^{13}C NMR spectra are quite similar. Similarities in chemical shifts carry over to the corresponding esters (**1e** and **2e**), as do the more shielded signals of **1e** (vs **2e**) for carbons 1, 2 and 4.

Conformation, Solution, and Chromatographic Properties. The ridge-tile, intramolecularly hydrogen-bonded conformation of bilirubin is well-established in nonpolar solvents such as $CHCl_3$. Vapor pressure osmometry (VPO) studies of mesobilirubins in $CHCl_3$ indicate monomers,[17,24] and ultracentrifugation equilibrium studies suggest aggregation[19] as the saturation limit of bilirubin is approached in $CHCl_3$. In contrast, the more $CHCl_3$ soluble diethyl ester of bilirubin has been shown by VPO to be

(18) (a) Boiadjiev, S. E.; Lightner, D. A. *J. Org. Chem.* **1997**, *62*, 399−404. (b) Boiadjiev, S.; Lightner, D. A. *J. Org. Chem.* **1998**, *63*, 6220−6228.

(19) Boiadjiev, S. E.; Watters, K.; Lai, B.; Wolf, S.; Welch, W. H.; McDonagh, A. F.; Lightner, D. A. *Biochemistry* **2004**, *43*, 15617−15632.

(20) Boiadjiev, S. E.; Lightner, D. A. *SYNLET* **1994**, 777−785.

(21) Chen, Q.; Huggins, M. T.; Lightner, D. A; Norona, W.; McDonagh, A. F. *J. Am. Chem. Soc.* **1999**, *121*, 9253−9264.

(22) Brower, J. O.; Lightner, D. A.; McDonagh, A. F. *Tetrahedron* **2001**, *57*, 7813−7827.

(23) Dey, S. K.; Lightner, D. A. *Monatsh. Chem.* **2007**, *138*, 687−697.

(24) (a) Brower, J. O.; Huggins, M. T.; Boiadjiev, S. E.; Lightner, D. A. *Monatsh. Chem.* **2000**, *131*, 1047−1053. (b) Boiadjiev, S. E.; Lightner, D. A. *J. Heterocyclic Chem.* **2000**, *37*, 863−870.

TABLE 1. ^{13}C NMR Chemical Shifts (δ, Ppm) of Tetramethoxybilirubin (1) and Tetraethylbilirubin (2), Their Diethyl Esters (1e and 2e) and 17-desmethyl-3,18-desvinyl-3,17-ethyl-18-methylbilirubin (=mesobilirubin-XIIIα, MBR) in $(CD_3)_2SO$ Solvent[a]

	carbon[b]	1	2	1e	2e	MBR[c]
1, 19	C=O	166.0	171. 7	166.0	171.6	171.9
2, 18	−C=	125.9	128.7	125.9	128.7	122.9
3, 17	−C=	146.3	146.8	146.4	146.7	147.1
4, 16	−C=	120.1	127.7	120.0	127.6	127.8
5, 15	−CH=	96.6	98.0	96.5	97.7	97.7
6, 14	−C=	121.4	122.0	121.3	121.8	122.4
7, 13	−C=	122.3	122.6	122.4	122.6	122.0
8, 12	−C=	119.1	119.3	118.8	118.9	119.3
9, 11	−C=	130.3	130.4	130.4	130.4	130.4
10	CH_2	23.5	23.5	23.6	23.6	23.3
$2^1/18^1$	CH_2, O, or CH_3	−	16.4	−	16.4	9.2
$2^2/18^2$	CH_3	60.2	13.9	60.3	13.9	−
$3^1/17^1$	CH_2 or O	−	17.0	−	17.0	17.2
$3^2/17^2$	CH_3	59.0	15.8	59.0	15. 8	14.8
$7^1/13^1$	CH_3	9.0	9.2	8.9	9.0	8.1
$8^1/12^1$	CH_2	19.2	19.3	19.4	19.2	19.2
$8^2/12^2$	CH_2	34.3	34.5	33.9	33.9	34.6
$8^3/12^3$	CO_2R	173.9	174.1	172.3	172.3	174.1
$8^3/12^3$	CO_2CH_2−	−	−	59.6	59.4	−
	$CO_2CH_2-CH_3$	−	−	13.9	13.9	−

[a] Assignments are based on gHSQC, *g*HMBC experiments, and NOE measurements. [b] For carbon numbering system, see Figure 1B. [c] Data from ref 22.

TABLE 2. Molecular Weights in $CHCl_3$ from Vapor Pressure Osmometry (VPO)[a] Measurements

compound	molecular wt (g/mol) MW[b]	formula wt (g/mol) FW
1	625 ± 13	624
2	613 ± 5	616
1e	1366 ± 57	680
2e	1364 ± 27	672

[a] The calibration standard was benzil: FW = 21 g/mol, MW 220 ± 15 g/mol. [b] Measured over a concentration range of 1.6−6.1 mol/kg.

dimeric at a concentration of $1-4 \times 10^{-3}$ and the dimers were shown by ^1H NMR to be intermolecularly hydrogen bonded.[10,24] The limited solubility of bilirubin itself in $CHCl_3$ has so far thwarted VPO studies of its molecular weight in solution. However, analogs with increased solubility, such as those with an *n*-butyl group on each lactam ring[17] or a C(10) *gem*-dimethyl group[24] have been shown to be monomeric.

In order to assess whether **1** and **2** are monomeric in $CHCl_3$ solution, we determined their molecular weights by vapor pressure osmometry (VPO).[24,25] The solution molecular weight of **1** was found to be 625 ± 13 g/mol and the molecular weight of **2** was 613 ± 5 g/mol (Table 2). Thus, both **1** and **2** are monomeric in $CHCl_3$ at or below the concentration range of the measurement. In contrast, the corresponding Rubin diethyl esters are dimers, consistent with the behavior of bilirubin esters as distinct from the acids. The differing behavior between acids and esters is apparently due to the ability of the acid to form a tightly knit set of 6 intramolecular hydrogen bonds, while the ester forms intermolecular hydrogen bonds between the dipyrrinone units.[10,26]

Visually similar to bilirubin, tetramethoxybilirubin **1** is a yellow solid that forms yellowish solutions; **2** is a bright yellow solid that also forms yellow solutions. Interestingly, while bilirubin is insoluble in CH_3OH (~0 μM),[27] **1** is soluble. Comparative solubility studies at saturation indicate for CH_3OH, **1**: 10.5 μg/mL, **2**: 1.6 μg/mL, bilirubin: ≤1.1 μg/mL; and for $CHCl_3$, **1**: 3.13 mg/mL, **2**: 1.01 mg/mL, bilirubin: 0.62 mg/mL. These measurements of solubility indicate that while **1** is at least 10 times more soluble in CH_3OH than bilirubin and **2**, it is 3-fold more soluble than **2** in $CHCl_3$, and **2** is approximately twice as soluble as bilirubin. Yet, **1** is less soluble in CH_3OH than in $CHCl_3$, by a factor of ~300. The data indicate that **1** is both more polar and more lipophilic than **2** and bilirubin.

TABLE 3. Comparison of the Dipyrrinone NH and Carboxylic Acid OH Chemical Shifts[a] of 1, 2 and Their Diethyl Esters (1e and 2e) with Those of Mesobilirubin-XIIIα (MBR) in $CDCl_3$ and $(CD_3)_2SO$ Solvents

	$CDCl_3$			$(CD_3)_2SO$		
pigments	lactam NH	pyrrole NH	CO_2H	lactam NH	pyrrole NH	CO_2H
1	10.22	9.00	13.12	9.56	10.26	11.86
2	10.59	9.14	13.67	9.78	10.32	11.91
MBR	10.57	9.15	13.62	9.72	10.27	11.87
1e	9.65	10.00	−	9.56	10.33	−
2e	10.25	10.30	−	9.73	10.41	−

[a] δ in ppm downfield from $(CH_3)_4Si$ for sample concentrations 4×10^{-3} M at 22 °C.

Chromatographic comparisons by TLC and HPLC indicate that **1** is more polar than **2** and bilirubin on silica gel TLC using 4% by vol. CH_3OH in CH_2Cl_2 as eluent: **1** has an $R_f \approx 0.74$, and **2** has an $R_f \approx 0.82$, and bilirubin exhibits an $R_f \approx 0.85$. In agreement with the greater polarity of **1**, the retention time of **1** (14 min) is faster than that of **2** (28 min) and bilirubin (18 min) on reverse phase HPLC. Although, like bilirubin, **1** and **2** are fully extracted from $CHCl_3$ into 5% aq. NaOH, consistent with intramolecular hydrogen bonding in both **1** and **2**, and similar to bilirubin, neither analog is extracted well into 5% (or saturated) aqueous sodium bicarbonate from chloroform: **1**, 11:89; **2**, 10:90; bilirubin 3:97 for bicarbonate:$CHCl_3$ partitioning from ~10^{-5} M solutions in $CHCl_3$. The methoxy groups of **1** clearly offer no advantage over the ethyl groups of **2** on the chloroform/bicarbonate partition coefficient. Taken collectively, these data suggest that while four methoxy groups of **1** do improve its aqueous solubility over that of bilirubin but not over **2**, they do render it more soluble than **2** by an order of magnitude and probably even more soluble than bilirubin in a polar hydroxylic solvent such as methanol.

Conformation from ^1H NMR Spectroscopy. A further good correlation with the picture of an intramolecularly hydrogen-bonded conformation in **1** may be found by ^1H NMR spectroscopy. The ^1H NMR spectrum of **1** in $CDCl_3$ reveals dipyrrinone NH deshieldings near 9.0 (pyrrole) and 10.2 (lactam) (Table 3), chemical shifts that are similar to those found in **2**, and in mesobilirubin-XIIIα and bilirubin. Such chemical shifts are characteristic of intramolecular hydrogen bonding to a carboxylic acid. Dipyrrinones are known to be avid participants in hydrogen bonding, preferably to carboxylic acids,[28,29] but also

(25) Huggins, M. T.; Lightner, D. A. *Monatsh. Chem.* **2001**, *132*, 203−221.

(26) Crusats, J.; Delgado, A.; Farrera, J.-A.; Rubires, R.; Ribó, J. M. *Monatsh. Chem.* **1998**, *129*, 741−753.

(27) Brodersen, R. *J. Biol. Chem.* **1979**, *254*, 2364−2369.

(28) (a) Boiadjiev, S. E.; Anstine, D. T.; Lightner, D. A. *J. Am. Chem. Soc.* **1995**, *117*, 8727−8736. (b) Boiadjiev, S. E.; Anstine, D. T.; Maverick, E.; Lightner, D. A. *Tetrahedron: Asymm.* **1995**, *6*, 2253−2270.

(29) (a) Huggins, M. T.; Lightner, D. A. *J. Org. Chem.* **2000**, *65*, 6001−6008. (b) Huggins, M. T.; Lightner, D. A. *Tetrahedron* **2001**, *57*, 2279−2287.

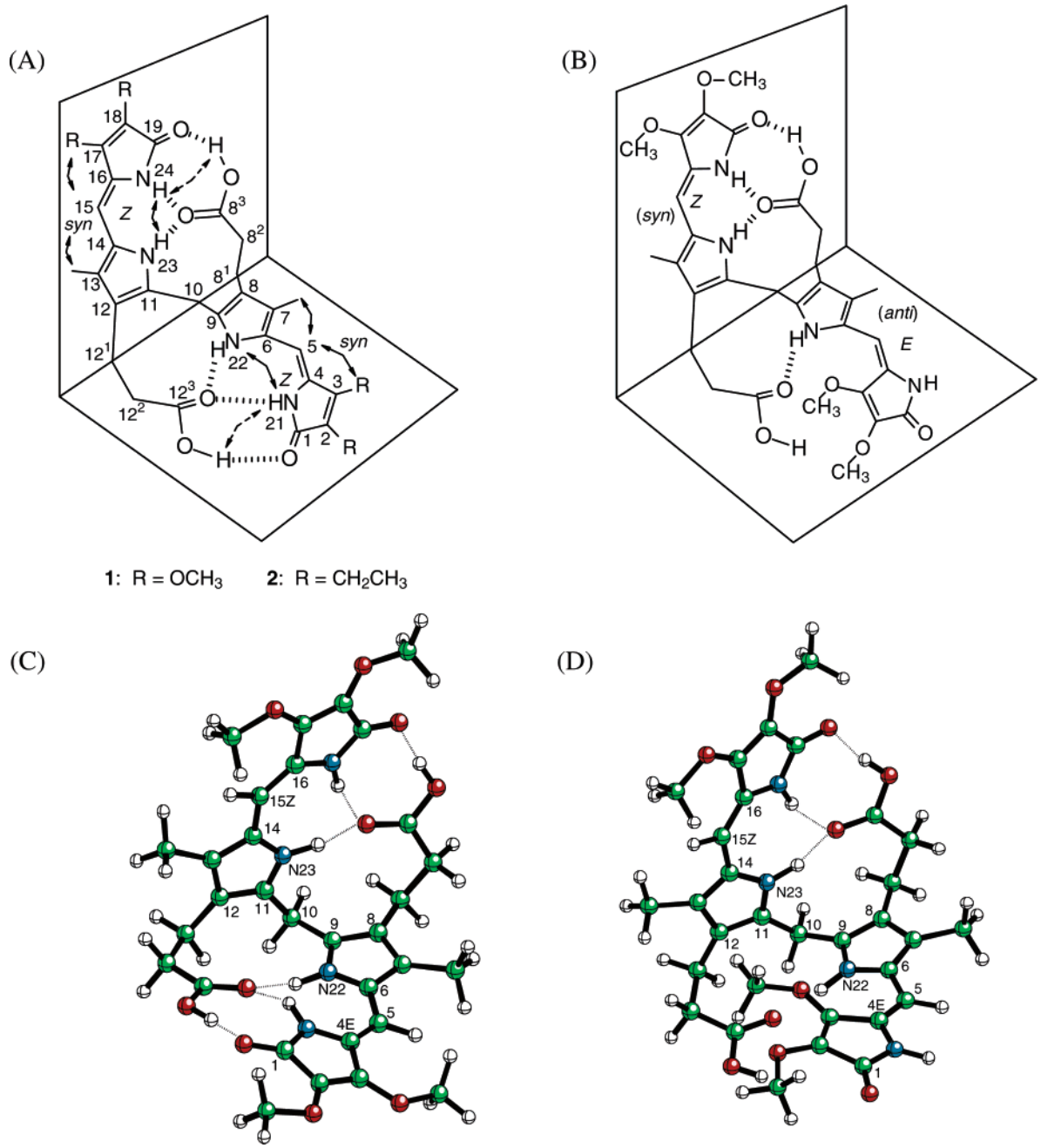

FIGURE 2. (A) Line drawings of intramolecularly hydrogen-bonded *syn*-(4*Z*,15*Z*)-**1** and *syn*-(4*Z*,15*Z*)-**2**, and (B) the *anti*-4*E*,*syn*-15*Z*-isomer of **1**. (A) Nuclear Overhauser effect correlations (curved arrows: strong, solid curve; weak, dashed curve) of tetramethoxybilirubin *Z*,*Z*-**1** and tetraethylbilirubin *Z*,*Z*-**2** in $CDCl_3$. (C) Ball and Stick representation of the energy-minimum conformations of (C) *syn*-*Z*,*Z*-**1** and (D) *anti*-*E*,*syn*-*Z*-**1**, as determined by molecular dynamics using the Sybyl forcefield (ref 40). In *Z*,*Z*-**1**, ϕ_1 ($N_{22}-C_9-C_{10}-C_{11}$) = 62°, ϕ_2 ($N_{23}-C_{11}-C_{10}-C_9$) = 62°, ψ_1 ($C_4-C_5-C_6-N_{22}$) = −21°, ψ_2 ($N_{23}-C_{14}-C_{15}-C_{16}$) = +17°. In *Z*,*Z*-**2**: $\phi_1 = 60°$, $\phi_2 = 61°$; $\psi_1 = -11°$, $\psi_2 = +10°$. In *E*,*Z*-**1**: $\phi_1 = 61°$, $\phi_2 = 53°$, $\psi_1 = -26°$, $\psi_2 = 23°$.

to each other (with association constants ∼25,000 M^{-1} in $CDCl_3$).[30] In $CDCl_3$, dipyrrinone *monomers* exhibit lactam and pyrrole NH chemical shifts of ∼8 ppm;[30b] whereas, intermolecularly hydrogen-bonded dipyrrinone dimers exhibit lactam and pyrrole NH chemical shifts ∼11 and ∼10 ppm, respectively. Dipyrrinones that are hydrogen bonded to CO_2H groups typically show lactam and pyrrole NH chemical shifts of ∼10.5 and ∼9 ppm, respectively.[28] The particular chemical shift (∼9 ppm) of the pyrrole NH seems to be diagnostic of dipyrrinone intramolecular hydrogen bonding to a carboxylic acid, and in Table 3 one finds a pyrrole chemical shift of 9.00 ppm for **1** as compared with the 9.14 ppm value seen in **2**. The deshielding of the CO_2H to 13.20 ppm provides added support to our conclusion that **1**, like **2**, is hydrogen bonded, a monomer, and adopts a bilirubin-like intramolecularly hydrogen-bonded conformation (Figure 2A).

Further support for the folded, intramolecularly hydrogen-bonded conformation is found from $^1H\{^1H\}$-homonuclear NOE experiments of **1** and **2** in $CDCl_3$. These showed the expected

(30) (a) Huggins, M. T.; Lightner, D. A. *Monatsh. Chem.* **2001**, *132*, 203−221. (b) Nogales, D. F.; Ma, J-S.; Lightner, D. A. *Tetrahedron* **1993**, *49*, 2361−2372.

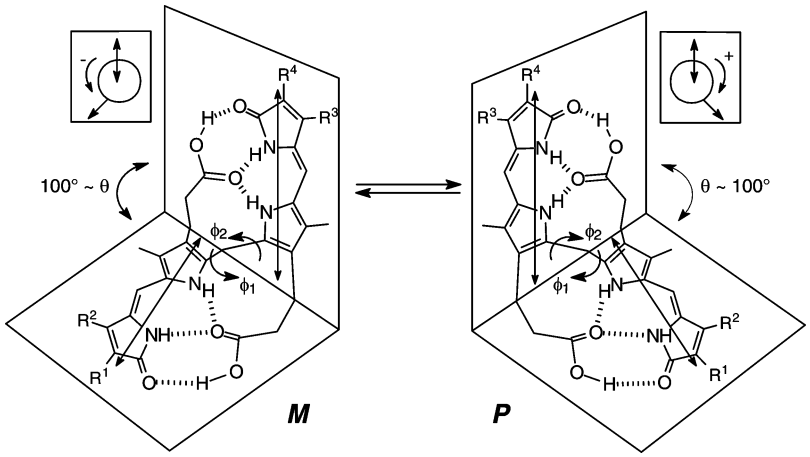

FIGURE 3. Ridge-tile shaped, folded intramolecularly hydrogen-bonded enantiomeric conformations (***M*** and ***P***) of bilirubin ($R^1 = R^3 = CH_3$, $R^2 = R^4 = CHCH_2$), *Z,Z*-**1** ($R^1 = R^2 = R^3 = R^4 = OCH_3$), and *Z,Z*-**2** ($R^1 = R^2 = R^3 = R^4 = CH_2CH_3$). Interconversion (M ⇄ P) is accomplished by rotating about ϕ_1 and ϕ_2. In ***M*** and ***P***, the dipyrrinone chromophores are planar, and the angle of intersection of the two planes (dihedral angle, θ) is ~100° for $\phi_1 \approx \phi_2 \approx 60°$. The double-headed arrows represent the approximate direction and intensity of the dipyrrinone long wavelength electric transition dipole moments. The relative orientations or helicities (***M***, minus; ***P***, plus) of the vectors are shown (inset) for each enantiomer. For these conformations the ***M*** dipole helicity correlates with the ***M*** molecular chirality and the ***P*** helicity with the ***P*** molecular chirality.

NOEs between the pyrrole and lactam NHs, and between the C(5,15) olefinic hydrogens and the C(7,13) methyls and C(3,-17) ethyls (Figure 2A). Only a faint NOE could be seen between the CO_2H and lactam NH of **1**, which might suggest weaker hydrogen bonding in **1** than in **2** or in bilirubin. In $(CD_3)_2SO$, both **1** and **2** exhibited many of the same NOEs seen in $CDCl_3$ and characteristic of the *syn-Z* configuration of the dipyrrinones.

The structure of Figure 2A, however, represents only one of two possible enantiomeric conformations, which, like bilirubin, interconvert (Figure 3) by breaking and remaking at least 3 hydrogen bonds in one dipyrrinone.[11] Consistent with this picture, the ^{1}H NMR spectra of **1** and **2** in $CDCl_3$ at 25 °C an ABCX pattern (see Figure 2C) is seen for the $-CH_2-CH_2-$ segment of the propionic acid chains, as it was in bilirubin:[31] **1**: $J_{AB} = 10.8$ Hz, $J_{AC} = 1.00$ Hz, $J_{AX} = -12$ Hz, $J_{BC} = -18$ Hz, $J_{BX} = 1.4$ Hz, $J_{CX} = 2.4$ Hz and **2**: $J_{AB} = 10.1$ Hz, $J_{AC} = 1.00$ Hz, $J_{AX} = -11$ Hz, $J_{BC} = -18$ Hz, $J_{BX} = 1.5$ Hz, $J_{CX} = 1.0$ Hz (obtained by computer simulation match). Which indicates that the conformational enantiomer interconversion rate is slow on the NMR time scale. As for bilirubin, coalescence may be observed upon warming. In $(CDCl_2)_2$ solvent, we observed coalescence at 95 °C for **1** and at 110 °C for **2**, and 105 °C for bilirubin.[31] The coalescence temperatures (T_c) correspond to a barrier, $\Delta G^{\ddagger} \approx 76.6$ kJ/mol for **1** and 79.9 kJ/mol for **2**, and 78.7 kJ/mol ($\Delta H^{\ddagger} = 74.1$ kJ/mol, $\Delta S^{\ddagger} = 2.5$ kJ/mol)[31] for bilirubin and a rate constant of interconversion, $k = 108$ s^{-1} for **1**, 106 s^{-1} for **2**, and 109 s^{-1} for bilirubin at T_c.

Conformation from UV-Visible Spectral Analysis. Additional evidence on the conformation of **1** and **2** comes from solvent-dependent UV−vis spectra. Over a wide range of solvents with varying polarity and hydrogen bonding ability (benzene, chloroform, acetone, methanol, acetonitrile and dimethylsulfoxide), the UV−vis spectra of **1** and **2** show similar solvent-dependence (see Table 2, Supporting Information), with broad absorption near 415 nm for **1** and 430 nm for **2** and a shoulder near 395 nm in most solvents. These long wavelength absorptions are probably exciton in nature and correspond to the two exciton components from electric dipole-electric dipole transition moment interaction of the two dipyrrinone chromophores.

In exciton coupling theory, the relative orientation of the relevant electric dipole transition moments is very important.[11,32] For dipyrrinones, this transition dipole lies along the long axis of the chromophore.[33,34] The dipyrrinones may rotate into a large number of relative orientations (conformations), and the planes encompassing each dipyrrinone are not co-incident; thus, the dipyrrinone electric dipole transition moments (Figure 3) have a chiral, helical relative orientation. For the "oblique" conformers, exciton coupling theory thus predicts intensity from both exciton transitions and hence a broadened UV−vis absorption curve. This is seen in the UV−vis spectra of both **1** and **2** in $(CH_3)_2SO$ solvent, where the location (λ) and shape of the UV−vis absorptions are very similar and little altered in going from polar $(CH_3)_2SO$ solvent to nonpolar solvents such as chloroform and benzene—an indication that the ridge-tile conformation (or more particularly the relative orientation of the dipyrrinone electric dipole transition moments) is scarcely altered with changes in solvents.

Induced Circular Dichroism. Bilirubins fold in the middle into ridge-tile conformations that lie at energy minima. With the added stabilization from intramolecular hydrogen bonding, two interconverting conformational enantiomers (Figure 3) dominate the conformational energy map.[11] In isotropic solvents, a 50:50 mixture of enantiomers obtains, but when a chiral complexation agent, such as quinine[34] or serum albumin,[35] is added, the equilibrium shifts toward either the ***M*** or ***P*** enantiomer, and in such cases one observes typically intense bisignate circular dichroism (CD) Cotton effects (Figure 4) for

(31) Navon G.; Frank, S.; Kaplan, D. *J. Chem. Soc., Perkin 2* **1984**, 1145−1149.

(32) Kasha, M.; El-Bayoumi, M. A.; Rhodes, W. *J. Chim. Phys.-Chim. Biol.* **1961**, *58*, 916−925.

(33) (a) Falk, H.; Vormayr, G.; Margulies, L.; Metz, S.; Mazur, Y. *Monatsh. Chem.* **1986**, *117*, 849−858. (b) Falk, H.; Grubmayr, K.; Höllbacher, G.; Hofer, O.; Leodolter, A.; Neufingerl, F.; Ribó, J. M. *Monatsh. Chem.* **1977**, *108*, 1113−1130.

(34) Lightner, D. A.; Gawroński, J. K.; Wijekoon, W. M. D. *J. Am. Chem. Soc.* **1987**, *109*, 6354−6362.

(35) Lightner, D. A.; Wijekoon, W. M. D.; Zhang, M. H. *J. Biol. Chem.* **1988**, *263*, 16669−16676.

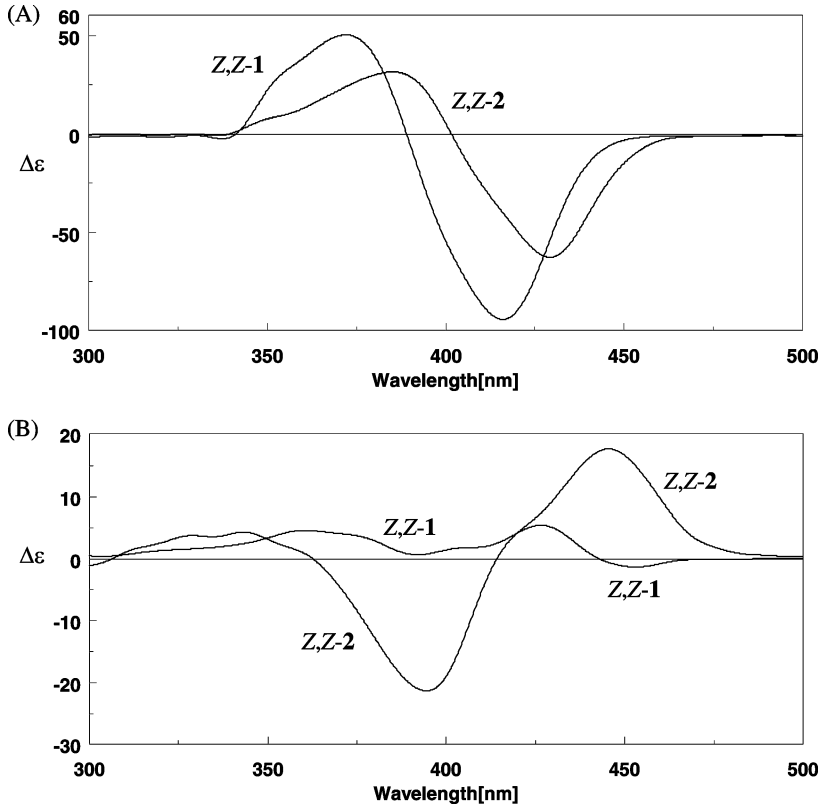

FIGURE 4. Comparison of the room-temperature circular dichroism (CD) and UV−visible spectroscopic data of *Z,Z*-**1** and *Z,Z*-**2** in (A) CH_2Cl_2 solutions containing quinine (pigment conc. ∼2×10^{-5} M; quinine conc. ∼6×10^{-3}; pigment:quinine molar ratio = ∼1:300) and in (B) aqueous HSA at pH 7.4 0.1 M tris buffer (pigment conc. ∼2×10^{-5} M, HSA conc. ∼4×10^{-5} M). In (A): *Z,Z*-**1**, $\Delta\epsilon_{372}^{max}$ +50, $\Delta\epsilon_{389} = 0$, $\Delta\epsilon_{416}^{max}$ −95; UV−vis ϵ_{418}^{max} 51 500 and *Z,Z*-**2**, $\Delta\epsilon_{385}^{max}$ +31, $\Delta\epsilon_{402} = 0$; $\Delta\epsilon_{429}^{max}$ −63; UV−vis ϵ_{433}^{max} 50 700. In (B), *Z,Z*-**1**, $\Delta\epsilon_{361}^{max}$ +4.4, $\Delta\epsilon_{427}^{max}$ +5.3; UV−vis ϵ_{403}^{max} 48 400 and *Z,Z*-**2**, $\Delta\epsilon_{394}^{max}$ −21, $\Delta\epsilon_{414} = 0$, $\Delta\epsilon_{446}^{max}$ +18; UV−vis ϵ_{415}^{max} 45 000.

TABLE 4. Circular Dichroism Data Following Microliter Additions of $CHCl_3$ to pH 7.4 Tris Buffered Aqueous HSA Solutions of 1 and 2[a]

μL $CHCl_3$ added	1			2		
	$\Delta\epsilon^{max}$ (λ_1)	$\Delta\epsilon = 0$ (λ_2)	$\Delta\epsilon^{max}$ (λ_3)	$\Delta\epsilon^{max}$ (λ_1)	$\Delta\epsilon = 0$ (λ_2)	$\Delta\epsilon^{max}$ (λ_3)
0	+4 (361)	−	+5 (427)	−21 (393)	411	+18 (446)
10	+17 (372)	391	−23 (415)	−11 (401)	−	−9 (423)
20	+28 (373)	391	−45 (417)	+5 (380)	396	−21 (427)
30	+33 (374)	391	−53 (417)	+9 (378)	396	−25 (427)
40	+34 (374)	391	−55 (417)	+14 (384)	399	−34 (428)
50	+34 (374)	391	−57 (417)	+10 (384)	401	−39 (429)
60	+34 (374)	391	−57 (417)	+21 (384)	401	−41 (429)
70	−	−	−			

[a] Tris buffer (0.1 M) with 2×10^{-5} M **1** + 4×10^{-5} M HSA (= human serum albumin) for **1** and **2**.

the long wavelength Rubin UV−vis electronic transitions near 400−450 nm. Such Cotton effects are associated with an exciton interaction between the Rubin's two dipyrrinone chromophores that are not directly conjugated.[11,34] And the signed order of the Cotton effects has been correlated with the relative orientation of the dipyrrinones and hence the absolute configuration ***M*** or ***P*** of the Rubin.[11,34]

As expected from earlier studies with bilirubin,[36] the weak CD Cotton effects from **2** on HSA are inverted and strengthened upon addition of small quantities of $CHCl_3$ (Table 4). Similarly, as anticipated from previous studies,[36] **1**, which exhibits even weaker CD Cotton effects when bound to HSA, gives strong CD signals upon addition of $CHCl_3$.

X-Ray Crystal Structure. Few X-ray crystal structures have been obtained of bilirubinoids,[8,9] stemming largely from considerable difficulties in growing crystals suitable for crystallography. The crystal structure of 4*Z*,15*Z*-bilirubin-IXα[9a] clarified and established the conformation of the pigment as shaped like a ridge-tile, with the propionic acids sequestered by the dipyrrinones by intramolecular hydrogen bonds (Figure 1C). Subsequently, crystal structures of the mesobilirubin-IXα-bis(chloroform),[9c] bilirubin chloroform-methanol solvate[9b] and di-isopropyl bilirubinate[9d] were obtained. More recently, crystal structures of a 10-thia-bilirubin,[37a] 10,10-spiro-bilirubins[37b] and a bilirubin ester[37c] were obtained. All crystal structures were of the 4*Z*,15*Z*-isomers. There are even fewer X-ray crystallographic studies of *E*-isomers. A double bond was shown to be inverted in a 5-nitro-biliverdin[38a] and to have the *E*-configuration in a 2,3-dihydrodipyrrinone with no β-substit-

(36) (a) Pu, Y. M.; McDonagh, A. F.; Lightner, D. A. *Experientia* **1992**, *48*, 246−248. (b) Pu, Y-M.; McDonagh, A. F.; Lightner, D. A. *J. Am. Chem. Soc.* **1993**, *115*, 377−380.

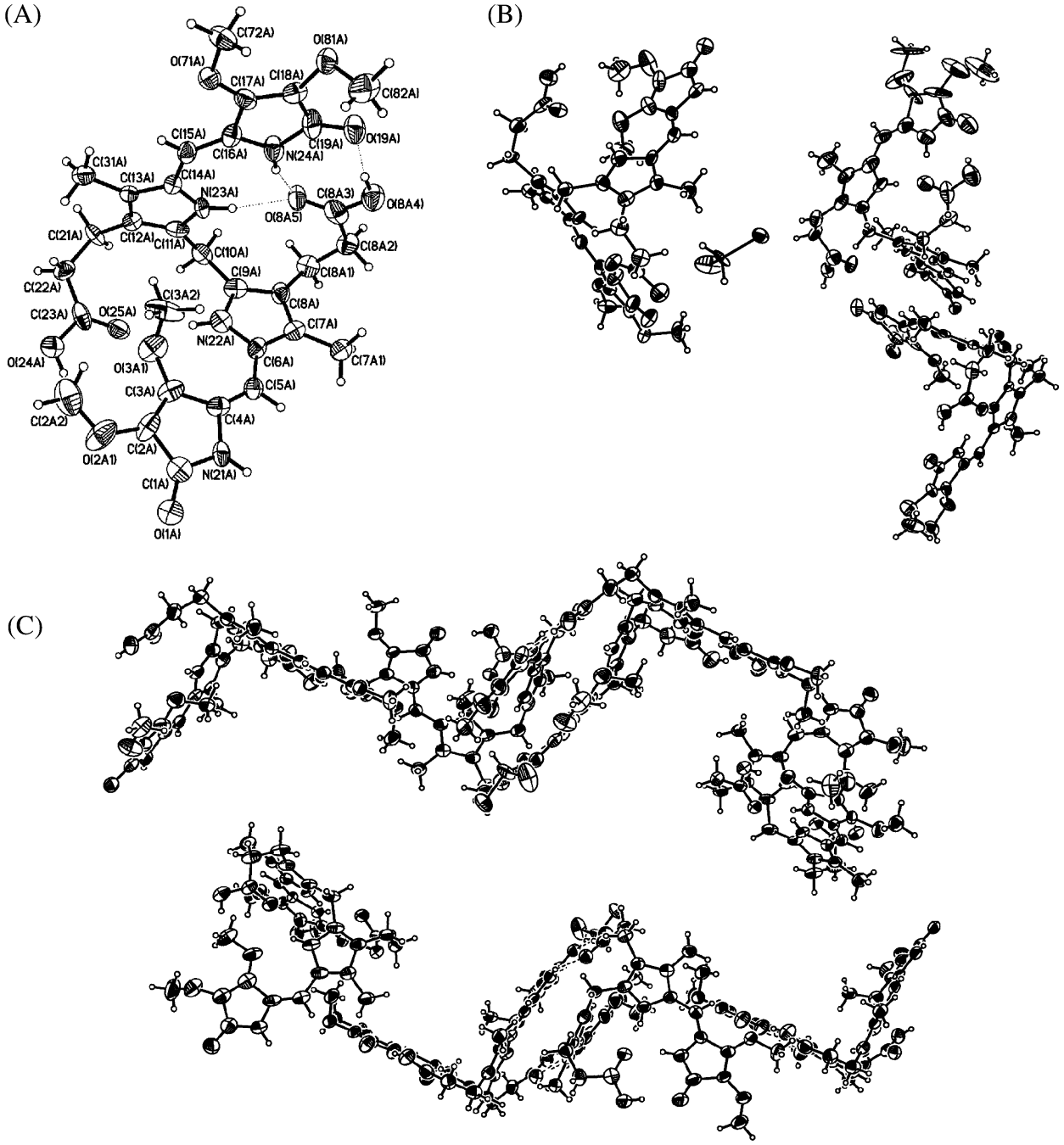

FIGURE 5. (A) Crystal structure drawing of the A-molecule in the crystal of 4*E*,15*Z*-**1**. (B) Unit cell of 4*E*,15*Z*-**1** showing 3 different molecules: A, B and C and a molecule of CH_2Cl_2. (C) Stacking of molecules A and B in the crystal. Compare the energy minimized structure of 4*E*,15*Z*-**1** from Sybyl molecular dynamics calculations (ref 40), see Figure 2D.

uents on the lactam ring[38b] and in a dipyrrinone obtained by photoisomerization of its *Z*-isomer.[38c] However, until now, there have apparently been no crystal structures of a 4*E*,15*Z* bilirubin isomer, the thermodynamically less stable diastereomer with the less stable double bond configuration, which is the isomer of great importance to the success of phototherapy for the jaundiced newborn.[1,2] *E*-isomers of bilirubin are generally unstable and inaccessible, except by irradiation with (blue) light.[2,39] We obtained crystals by slow diffusion of *n*-hexane into a CH_2Cl_2 solution of 4*E*,15*Z*-**1** in dim (white) light. Expecting the crystals to be of the 4*Z*,15*Z* isomer, we were surprised to observe a structure corresponding to the *E*-isomer (Figure 5).

(37) (a) Tipton, A.; Lightner, D. A. *Monatsh. Chem.* **2002**, *133*, 707−716. (b) Ghosh, B.; Catalano, V. J.; Lightner, D. A. *Monatsh. Chem.* **2004**, *135*, 1305−1317. (c) Ghosh, B.; Catalano, V. J.; Lightner, D. A. *Monatsh. Chem.* **2004**, *135*, 1503−1517.

(38) (a) Bonfiglio, J. V.; Bonnett, R.; Buckley, D. G.; Hamzetash, D.; Hursthouse, M. B.; Abdul Malik, K. M.; Naithani, S. C.; Trotter, J. *J. Chem. Soc., Perkin 1* **1982**, 1291−1982. (b) Sheldrick, W. S.; Borkenstein, A.; Blacha-Puller, M.; Gossauer, A. *Acta Crystallogr.* **1977**, *B33*, 3625−3635. (c) Hori, A.; Mangani, S.; Meyer, E. F., Jr.; Cullen, D. L.; Falk, H.; Grubmayr, K. *J. Chem. Soc., Perkin 2* **1981**, 1525−1528.

(39) (a) McDonagh, A. F.; Palma, L. A.; Trull, F. R.; Lightner, D. A. *J. Am. Chem. Soc.* **1982**, *104*, 6865−6867. (b) McDonagh, A. F.; Palma, L. A.; Lightner, D. A. *J. Am. Chem. Soc.* **1982**, *104*, 6867−6869.

TABLE 5. Conformation of the Two Propionic Acid Groups in *E,Z*-1 from X-ray Structure[a] and Molecular Dynamics Calculations[b]

torsion angle (deg)	propionic acid at C(8)	propionic acid at C(12)	torsion angle (deg)
C(9A)−C(8A)−C(8A1)−C(8A2)[a]	123.2	113.7	C(11A)−C(12A)−C(21A)−C(22A)
C(9)−C(8)−C(8^1)−C(8^2)	119.8	107.4	C(11)−C(12)−C(12^1)−C(12^2)
C(8A)−C(8A1)−C(8A2)−C(8A3)[a]	−59.0	−74.9	C(12A)−C(21A)−C(22A)−C(23A)
C(8)−C(8^1)−C(8^2)−C(8^3)[b]	−71.8	−67.6	C(12)−C(12^1)−C(12^2)−C(12^3)
C(8A1)−C(8A2)−C(8A3)−O(8A5)[a]	−15.1	−5.3	C(21A)−C(22A)−C(23A)−O(25A)
C(8^1)−C(8^2)−C(8^3)═O[b]	16.9	−1.0	C(12^1)−C(12^2)−C(12^3)═O
C(8A1)−C(8A2)−C(8A3)−O(8A4)[a]	166.4	175.5	C(21A)−C(22A)−C(23A)−O(24A)
C(8^1)−C(8^2)−C(8^3)−OH[b]	−166.1	178.9	C(12^1)−C(12^2)−C(12^3)−OH

[a] Numbering according to Figure 5. [b] Corresponding torsion angles using the standard numbering system (Figure 1C).

TABLE 6. Comparison of Hydrogen Bond and Main Atom Nonbonded Distances (Å)[a] between Propionic Acids and Dipyrrinones in *E,Z*-1 with Bilirubin, *Z,Z*-1 and *Z,Z*-2

hydrogen bond and main atom nonbonded distance (Å)	*E,Z*-**1**[b] crystal A	*E,Z*-**1**[b] crystal B	*E,Z*-**1**[b] crystal C	bilirubin[c] crystal	molecular dynamics[d] *E,Z*-**1**	molecular dynamics[d] *Z,Z*-**1**	molecular dynamics[d] *Z,Z*-**2**
(*Z*) L−N−H···O═C−A[e]	1.946	1.920	1.892	1.75	1.640	1.627/1.601	1.547/1.543
(*Z*) L−N to O═C−A[f]	2.787	2.728	2.732	2.80	2.581	2.562	2.540
(*E*) L−N to O═C−A[g]	5.852	5.737	5.760	2.80	5.177	2.553	2.539
(*Z*) P−N−H···O═C−A[e]	2.197	2.026	2.073	1.78	1.602	1.560	1.579
(*Z*) P−N to O═C−A[f]	3.002	2.882	2.889	2.81	2.552	2.542	2.583
(*E*) P−N−H···O═C−A[h]	2.457	2.413	2.495	−	1.679	−	−
(*E*) P−N to O═C−A[g]	3.172	3.089	3.189	2.81	2.521	2.549	2.616
(*Z*) A−OH···O═C−L[e]	1.814	1.847	1.800	1.52	1.575	1.513	1.543
(*Z*) A−HO to O═C−L[i]	2.641	2.703	2.632	2.53	2.460	2.471	2.495
(*E*) A−HO to O═C−L[i]	7.090	7.020	6.624	2.53	5.742	2.453	2.483

[a] L = lactam, P = pyrrole, A = carboxylic acid. [b] From the crystallographic structure of this work. [c] From the atomic coordinaters of ref 9a. [d] Molecular dynamics using Sybyl (ref 40). [e] Hydrogen bond distances from the *syn-Z*-configuration dipyrrinone to the C(8) propionic acid. [f] Main atom nonbonded distances between the C(12) acid (A) carbonyl oxygen and lactam (L) or pyrrole (P) nitrogen of the *syn-Z*-configuration dipyrrinone. [g] Main atom nonbonded distances between the C(8) acid (A) carbonyl oxygen and lactam (L) or pyrrole (P) nitrogen of the *anti-E* dipyrrinone. [h] Hydrogen bond distance from the *anti-E*-configuration dipyrrinone pyrrole NH. [i] Main atom nonbonded distances between the *Z*- or *E*-configuration lactam (L) carbonyl oxygen and the proximal acid (A) OH oxygen.

The crystal of 4*E*,15*Z*-**1** shows three different molecules in the unit cell: A, B and C. All three are *E*-isomers of only slightly different geometry. Molecule A (as well as B and C) shows an inverted *E*-configuration C(4)−C(5) carbon−carbon double bond with an *anti*-conformation of the dipyrrinoen (Table 6 and Figure 2). The C(15)−C(16) double bond configuration is *Z*, and the *Z*-configuration dipyrrinone retains the *syn* geometry required for intramolecular hydrogen bonding with the C(8) propionic acid—the propionic acid stemming from C(8) on the *E*-configuration dipyrrinone. A ridge-tile-like conformation of the molecule is nonetheless maintained, consistent with earlier work that indicated the ridge-tile is the energetically most stable, aside from any intramolecular hydrogen bonding.[11] The C(12) propionic acid group, uncoupled from hydrogen bonding to its (now *E*-configuration) dipyrrinone, still remains in a position similar to that in *Z,Z*-**1**, i.e., as may be judged from the torsion angles in the C(12)−CH_2−CH_2−CO_2H segment, which are very close to those of C(8)−CH_2−CH_2−CO_2H (Table 5). There is no large relocation of the former in *E,Z*-**1** and it remains tucked inward toward the concave surface of the tetrapyrrole skeleton as in *Z,Z*-**1**. However, while this CO_2H group is too far distant from the *E*-dipyrrinone for any hydrogen bonding to the lactam residue. This is clear from the large nonbonded distance between the *E*-dipyrrinone lactam nitrogen and C(12) acid carbonyl oxygen (∼5.8 Å) and acid OH oxygen (∼7 Å) as compared with the corresponding distances (∼2.8 and ∼2.6 Å, respectively, from the *Z*-dipyrrinone and the C(8) acid (Table 6). However, in the *E*-configuration dipyrrinone the pyrrole nitrogen to C(12) acid carbonyl oxygen (∼3.1 Å) distance is only slightly longer than that between the *Z*-dipyrrinone nitrogen and the C(8) acid (∼2.9 Å), and the distance is only slightly longer than the sum (2.9 Å) of the van der Waals radii of N (1.5 Å) and O (1.48 Å). Thus, a weak hydrogen bond of the pyrrole NH···O═C type may be present.

The *E*-dipyrrinone half of *E,Z*-**1** is not especially distorted from planarity. Presumably, nonbonded steric repulsions would arise between the *β*-methoxy groups and the C(7)-CH_3 if the *anti-E*-dipyrrinone were rotated about the C(5A)−C(6A) bond to produce the *syn-E* conformation. In the *anti*-conformation, the *E*-dipyrrinone adopts a nearly planar shape, with small torsion angles about C(5): the C(4)═C(5) double bond is twisted slightly, 8−11°, in molecules A, B and C; and the C(4)═C(5)−C(6)-N(22) torsion angle is twisted by only 10−16° (Table 7). These torsion angles compare favorably to the corresponding torsion angles in the intramolecularly hydrogen-bonded *Z*-configuration dipyrrinone component: C(14)−C(15)−C(16)−N(24) = ∼1−7° and N(23)−C(14)−C(15)═C(16) = ∼1−7°. They are not very different from those (Table 7) found in the X-ray crystal structure of bilirubin itself. But they differ in one major way from the structure of the simple *anti-E*-dipyrrinone, 4(*E*)-2,3-dimethyldipyrrin-2-one, whose X-ray crystal structure shows the *anti-clinal* conformation, with a C(4)−C(5)−C(6)−N(2) torsion angle of 49.8°—or much larger than the 10−16° torsion angle seen in *E,Z*-**1**. Whether the difference is due to a stacking phenomenon in the crystal or to the presence of the proximal C(12) propionic acid is unclear. And so the shape of the *E,Z*-**1** pigment is a ridge tide and rather like that of 4*Z*,15*Z*-bilirubin-IXα, with comparable torsion angles about the middle, C(10), [N(22)−C(9)−C(10)−C(11) and C(9)−C(10)−C(11)−N(23)] and comparable dihedral angles (*θ*) between the average planes of the two dipyrrinones (Table 7).

TABLE 7. Comparison of Torsion and Dihedral Angles in Crystals of 4*E*,15*Z*-tetramethoxy-bilirubin (*E*,*Z*-1) for the Three Molecules of the Unit Cell with Those Computed for *Z*,*Z*-1 and *Z*,*Z*-2

	E,*Z*-**1**				molecular dynamics[c]		
torsion angle (deg)[a]	A	B	C	bilirubin[b]	*E*,*Z*-**1**	*Z*,*Z*-**1**	*Z*,*Z*-**2**
N(21)−C(4)═C(5)−C(6)	170.2	−169.2	−172.1	−5.8	178.5	−0.9	−0.8
C(4)═C(5)−C(6)−N(22) = ψ_1	15.9	10.6	10.3	17.5	−25.5	−20.6	−10.5
N(22)−C(9)−C(10)−C(11) = ϕ_1	−59.0	−58.2	56.6	59.8	60.8	61.9	60.1
C(9)−C(10)−C(11)−N(23) = ϕ_2	−46.5	−55.2	53.2	63.7	52.7	61.5	61.0
N(23)−C(14)−C(15)═C(16) = ψ_2	−6.5	1.0	4.0	−2.7	22.6	17.3	9.9
C(14)−C(15)═C(16)−N(24)	−2.5	6.6	1.4	10.7	1.1	1.1	1.1
interplanar dihedral angle (θ)	96[d]	83[d]	88[d]	95/99[e]	91[d]	88[d]	92[d]
	96[f]	90[f]	95[f]	98/83[f]	94[f]	90[f]	92[f]

[a] For ϕ, ψ, θ angles, see Figures 2 and 3. [b] Data from ref 9a and its atomic coordinates. [c] Molecular dynamics using Sybyl (ref 40). [d] Interplanar angle of intersection of the average planes of the two dipyrrinones. [e] Two molecules in the unit cell. [f] Interplanar angle of intersection of the two pyrrole rings.

In other aspects, there is nothing particularly different among key bond distances and bond angles in the *E*- and *Z*-dipyrrinones. In the *E* the lactam C═O distance is 1.237 Å, in the *Z* it is 1.253 Å; in the *E* the C(4)═C(5) double bond distance is 1.35 Å, in the *Z* C(15)═C(16) is 1.364 Å; in the *E* the C(5)−C(6) distance is 1.407 Å, in the *Z* the C(14)−C(15) distance is 1.429 Å. And the C(4)−C(5)−C(6) bond angle is 130.8° in the *E*; or nearly identical to the C(14)−C(15)−C(16) = 130.6° in the *Z*.

In the ridge-tile conformation, *E*,*Z*-**1** is "half hydrogen bonded," but all of the hydrogen bond distances lactam and pyrrole N−H to acid O═C, and acid OH to lactam O═C are ∼0.2 to 0.3 Å longer than those of bilirubin (Table 6). The data indicate a small distortion about the middle, C(10), that apparently perturbs the ridge-tile making the remaining 3 intramolecular hydrogen bonds of *E*,*Z*-**1** longer and probably less stabilizing. If one could study the conformational interconversion rates of *E*,*E*-**1**, from one ridge-tile to its enantiomer, one might expect lower barriers and faster rates compared to *Z*,*Z*-**1**, *Z*,*Z*-**2** and bilirubin.

Conformation Analysis from Molecular Dynamics. Independent rotations of the approximately planar, thermodynamically most stable *syn*-*Z*-dipyrrinones of **1** or **2** about the central CH_2 lead to an infinite number of conformations, including two high-energy limiting cases where the dipyrrinones lie nearly coplanar: porphyrin-like and linear (Figures 1A and B). Lying between these extremes is a conformation stabilized by intramolecular hydrogen bonding (Figure 1C). The energy-minimum conformation of **1** and **2**, as determined by molecular dynamics using the Sybyl forcefield,[40] gave a conformation in which both propionic acid groups are engaged in intramolecular hydrogen bonding to an opposing dipyrrinone (Figure 2A). In the energy-minimized structures of *Z*,*Z*-**1** (Figure 2C) and *Z*,*Z*-**2**, the extended planes of the dipyrrinones of each intersect at C(10) with dihedral angles of ∼88° and ∼92°, respectively, for (ϕ_1, ϕ_2) angles of 62°, 62°) and (60°, 61°), respectively, and essentially the same as those seen in bilirubin-IXα and mesobilirubin-XIIIα. The dipyrrinone units in each compound remain relatively planar, with C(4)═C(5)−C(6)−N(22) and N(23)−C(14)−C(15)═C(16) torsion angles of 17° and −21° in *Z*,*Z*-**1**, and 10° and −11° in *Z*,*Z*-**2** (Table 7). These values are not very different from those computed for *E*,*Z*-**1** (Figure 2D), which indicate approximately coplanar dipyrrinones, both in the intramolecularly hydrogen-bonded *syn*-*Z* and in the non-hydrogen-bonded *anti*-*E*. A residual hydrogen bond between the pyrrole of the *E*-configuration dipyrrinone of *E*,*Z*-**1** and the propionic acid attached to C(12) may be detected in the energy-minimized structure — as it is in the crystal. The computed overall tetrapyrrole geometry of *Z*,*Z*-**1** and *Z*,*Z*-**2** matches up well with those computed for 4*Z*,15*Z*-bilirubin-IXα and 4*Z*,-15*Z*-mesobilirubin-XIIIα and those found in their crystals (Table 7). No unusual effects are seen by replacing the lactam β-alkyl group with methoxyls. The computed overall geometry of *E*,*Z*-**1** (Figure 2D) matches well with that from its X-ray structure (Figure 5).

Concluding Comments

Our first attempt to prepare an amphiphilic bilirubin with ether groups at all lactam β-positions led to 4*Z*,15*Z*-**1**, which showed considerably improved solubility in CH_3OH over bilirubin. It also paved the way to our obtaining the first X-ray crystal structure of a bilirubin *anti*-*E*-isomer, which, despite the inverted double bond, still maintains the ridge-tile shape.

Experimental Section

General Procedures. General procedures were given previously.[11,17,21,24,35] Nuclear magnetic resonance (NMR) spectra were obtained at 400 MHz unless otherwise noted, or at 500 MHz spectrometer. HSQC, gHMBC and NOE NMR were obtained at 500 MHz. Chemical shifts were reported in δ ppm referenced to the residual $CHCl_3$ ^1H signal at 7.26 ppm and ^{13}C at 77.23 ppm. Analytical thin layer chromatography (TLC) was carried out on silica gel IB−F plates (125 μm layers). Flash column chromatography was carried out using silica gel, 60−200 mesh. Radial chromatographic purification was achieved on 1, 2 or 4 mm thickness silica gel PF_{254} with $CaSO_4$ binder. HPLC analyses were carried out with detector at 410 on ultrasphere-IP 5 μm C-18 ODS column (25 × 0.46 cm) fitted with a similarly packed precolumn (4.5 × 0.46 cm). The flow rate was 0.75−1.0 cm^3/minute; the elution solvent was 0.1 M di-*n*-octylamine acetate in 5% aqueous CH_3OH, the column temperature was ∼34 °C. Spectroscopic data were obtained in spectral grade solvents. Dipyrrylmethane dialdehyde **3**,[17] 3,4-dimethoxypyrrolin-2-one (**4**)[23] and 3,4-diethyl-3-pyrrolin-2-one (**5**)[16] were synthesized according to previously published methods.

(4*Z*,15*Z*)-2,3,17,18-Tetramethoxymesobilirubin-XIIIα (1). To a solution of dipyrrole dialdehyde **3**[17] (500 mg, 1.60 mmol) and pyrrolinone **4**[23] (1.33 mmol, 9.3 mmol, 8 mol equiv.) in methanol (20 mL) was added 20 mL of 6 M aq. KOH under N_2. The mixture was stirred at reflux for 120 h, with repeated checking by TLC. The solution was cooled to 0 °C and acidified slowly using saturated

(40) The molecular dynamics calculations used to find the global energy minimum conformations of **1** were run on an SGI Octane workstation using vers. 7.1 of the Sybyl forcefield as described in ref 11. The Ball and Stick drawings were created from the atomic coordinates using Müller and Falk's "Ball and Stick" program for the Macintosh (http://www.orc.uni-Linz.ac.at/mueller/ball_stick.html).

$NaHSO_4$ solution. The acidified solution was extracted with CH_2Cl_2 (5 × 100 mL), and the CH_2Cl_2 extract was dried (anhyd Na_2SO_4) and evaporated (rotovap) to yield a yellow-orange solid. Trituration with cold CH_3OH dissolved the orange tripyrrole intermediate, leaving behind pure yellow product **1**, 85 mg, 13% yield, or 44% based on recovered tripyrrole intermediate. It had mp 250 °C (dec); IR (KBr) ν 3151, 2253, 1698, 1468, 1381, 1096, 908, 735 cm^{-1}; ^1H NMR ($CDCl_3$, 500 MHz) δ 2.13 (s, 6H), 2.50−3.01 (m, 8H), 3.85 (s, 6H), 4.02 (s, 2H), 4.09 (s, 6H), 6.16 (s, 2H), 8.99 (s, 2H), 10.22 (s, 2H), 13.12 (brs, 2H) ppm; ^1H NMR (DMSO-d_6, 500 MHz) δ 1.10 (t, J = 7.5 Hz, 6H), 1.79 (s, 6H), 2.07 (s, 6H), 2.37 (t, J = 7.5 Hz, 4H), 2.53 (q, J = 7.5 Hz, 4H), 2.69 (t, J = 7.5 Hz, 4H), 5.93 (s, 2H), 10.11 (brs, 2H), 11.18 (brs, 2H) 12.14 (brs, 2H) ppm; ^{13}C NMR data are in Table 1 and UV−vis data are in Table 2 of the Supporting Information. Anal. Calcd for $C_{31}H_{36}N_4O_8$ (624.7): C, 59.61; H, 5.81; N, 8.97. Calcd. for $C_{31}H_{36}N_4O_8 \cdot 1/2H_2O$ (633.7): C, 58.76; H, 5.89; N, 8.84. Found: C, 58.60; H, 5.88, N, 8.83.

(4*Z*,15*Z*)-2,3,17,18-Tetramethoxymesobilirubin-XIIIα Diethyl Ester (1e). To a solution of dipyrrole-dialdehyde **3** (350 mg, 0.81 mmole) and dimethoxypyrrolinone **4** (0.466 gm, 3.26 mmol, 4 mol eq) in 5 mL of dry acetonitrile and 2 mL of dry toluene in a pressure tube was added 0.6 mL of DBU. The pressure tube was sealed under N_2 atmosphere and heated at 120−140 °C for 96 h. The reaction mixture was diluted with CH_2Cl_2, washed with 5% aq. HCl (2 × 50 mL) and then with water (2 × 50 mL). The organic layer was dried and evaporated (rotovap). The residue was first purified by flash chromatography using 2% MeOH in CH_2Cl_2 on silica gel and then by radial chromatography using a 5:2 to 1:2 hexane:ethyl acetate gradient as eluent. The pure fractions were combined and evaporated to obtain 40 mg of pure diethyl ester **1e**. It had mp 132 °C (melted with dec); IR (KBr) ν 3151, 2982, 2254, 1685, 1473, 1381, 1096, 908, 734 cm^{-1}; ^1H NMR ($CDCl_3$, 500 MHz) δ 10.00 (brs, 2H), 9.65 (brs, 2H), 6.12 (s, 2H), 4.15 (q, J = 7.5 Hz, 4H), 4.08 (s, 2H), 4.01 (s, 6H), 3.47 (s, 6H), 2.83 (t, J = 7.5 Hz, 4H), 2.41 (t, J = 7.5 Hz, 4H), 2.05 (s, 6H), 1.26 (t, J = 7.5 Hz, 6H) ppm; ^{13}C NMR ($CDCl_3$,500 MHz) δ 173.5, 168.7, 147.3, 131.3, 126.9, 123.7, 123.0, 121.4, 118.8, 100.4, 60.6, 59.4, 35.9, 20.2, 14.5, 9.8 ppm. *Anal*. Calcd for $C_{35}H_{44}N_4O_8$ (680.8): C, 61.75; H, 6.52; N, 8.23. Calcd for $C_{35}H_{44}N_4O_8 \cdot 1/2H_2O$ (689.8): C, 60.94; H, 6.57; N, 8.12. Found: C, 60.81; H, 6.54; N, 8.15.

(4*Z*,15*Z*)-2,3,17,18-Tetraethylmesobilirubin-XIIIα Diethyl Ester (2e). To a solution of dipyrryl dialdehyde **3** (320 mg. 0.75 mmol) and diethyl pyrrolinone **5** (414 mg, 2.98 mmoles, 4 mol eq) in 30 mL of dry toluene in a round-bottom flask was added 0.6 mL of phosphazene P_1-*t*-butyl base, and the reaction mixture was heated at reflux for 72 h under N_2. The toluene was evaporated (rotovap), and the residue was dissolved in CH_2Cl_2, washed with 5% aq. HCl (2 × 50 mL) followed by water (2 × 50 mL). The organic layer was dried, evaporated (rotovap) and the residue was purified by radial chromatography using a 5:2 to 1:1 hexane:ethyl acetate gradient as eluent. The pure fractions were evaporated (rotovap) to yield 115 mg of desired diethyl ester (**2e**) in 23% yield. It had mp 206−207 °C (corrected); IR (KBr) ν 3151, 2982, 2254, 1685, 1466, 1381, 1096, 908, 735 cm-;[1] ^1H NMR ($CDCl_3$, 500 MHz) δ 10.30 (brs, 2H), 10.25 (brs, 2H), 5.92 (s, 2H), 4.15 (q, J = 7.0 Hz, 4H), 4.12 (s, 2H), 2.87 (t, J = 7.5 Hz, 4H), 2.44 (t, J = 7.5 Hz, 4H), 2.36 (q, J = 7.5 Hz, 4H), 2.08 (s, 6H), 2.00 (q, J = 7.5 Hz, 4H), 1.27 (t, J = 7.0 Hz, 6H), 1.05 (t, J = 7.5 Hz, 6H), 0.80 (t, J = 7.5 Hz, 6H) ppm; ^{13}C NMR ($CDCl_3$, 125 MHz) δ 174.0, 173.6, 146. 9, 131.1, 129.6, 129.3, 124.1, 122.6, 118.9, 100.5, 60.6, 36.0, 22.7, 20.3, 17.9, 16.8, 15.9, 14.5, 13.9, 9.9 ppm. *Anal*. Calcd for $C_{37}H_{48}N_4O_6$ (672.9): C, 69.62; H, 7.79; N, 8.33. Calcd for $C_{37}H_{48}N_4O_6 \cdot 1/2H_2O$ (681.9): C, 68.70; H, 7.83; N, 8.22. Found: C, 68.80; H, 7.66; N, 8.05.

UV and CD Measurements. Stock solutions of **1** and **2** (∼7.0 × 10^{-4} M) were prepared by dissolving an appropriate amount of the desired pigment in 0.5 mL of DMSO and $CHCl_3$. Next, a 100 μL aliquot of the stock solution was diluted to 5 mL (volumetric flask) the specified organic solvent for UV−vis studies (Table 3) or, for CD studies involving human serum albumin (HSA), with an HSA solution (∼4 × 10^{-5} M in pH 7.4 Tris buffer).[35] The final concentration of the solution was ∼2 × 10^{-5} M in pigment. Up to four 5 mL solutions of each pigment were prepared, as needed, in 5 mL volumetric flasks. For CD studies in $CHCl_3$, solutions were prepared directly in $CHCl_3$ containing a 300:1 molar ratio of quinine:pigment to give final concentrations of ∼2 × 10^{-5} M in pigment.

Acknowledgment. We thank the National Institutes of Health (HD-17779) for generous support of this work, the National Science Foundation (CHE-0226402 and CHE-0521191) for providing funding for the purchase of the X-ray diffractometer used in this work and for acquisition of a 400 MHz NMR spectrophotometer and upgrade of our 500 MHz NMR. We also thank Dr. N. T. Salzameda for assistance in obtaining the crystal structure data, Prof. T. W. Bell for use of the vapor pressure osometer, and Prof. A. F. McDonagh for running the HPLCs. S.K.D. is an R.C. Fuson Graduate Fellow.

Supporting Information Available: UV−vis data, NMR spectra, and X-ray experimental data. This material is available free of charge via the Internet at http://pubs.acs.org.

JO702593X